Available online at www.sciencedirect.com
SCIENCE DIRECT®
Journal of Solid State Chemistry 178 (2005) 3020–3026
JOURNAL OF SOLID STATE CHEMISTRY
www.elsevier.com/locate/jssc

Exchange interactions in $R_2Fe_{17-x}Ga_x$ (R = Y, Sm, Gd, Tb, Ho and Tm) compounds

Fumio Maruyama*

Department of Physics, Faculty of Science, Shinshu University, Matsumoto 390-8621, Japan

Received 23 May 2005; received in revised form 4 July 2005; accepted 6 July 2005
Available online 22 August 2005

Abstract

We calculated the molecular field coefficients, n_{FeFe} and n_{RFe} (R = Sm, Gd, Tb, Ho and Tm), for $R_2Fe_{17-x}Ga_x$ and the values of n_{FeFe} and n_{SmFe} for $R_2Fe_{17-x}T_x$ (T = Al and Si) using the experimental values of the Curie temperature. The values of n_{FeFe} increase in spite of the decrease of μ_{Fe} for $0 \leqslant x \leqslant 5$. The values of n_{SmFe} have large values when the magnetic anisotropy is axial. For $6 \leqslant x \leqslant 8$, the values of n_{FeFe}, n_{HoFe} and n_{TmFe} increase largely, which is related to the change of the easy magnetization direction. For $Y_2Fe_{17-x}T_x$ (T = Ga and Al), the values of n_{FeFe} have a maximum value with increasing those of μ_{Fe}. With increasing V^{-1}, the values of n_{FeFe} have a maximum value around the same value of V^{-1} for $Y_2Fe_{17-x}T_x$ (T = Ga and Al). For $Y_2Fe_{17-x}Si_x$, the values of n_{FeFe} increase with increasing V^{-1}.

Keywords: Magnetically ordered materials; Magnetic properties; Exchange interactions

1. Introduction

In rare-earth–transition metal (R–M) compounds, three types of exchange interactions occur: M–M, R–M and R–R. In general, for compounds where the transition metal atoms carry a well-established magnetic moment, the M–M interaction dominates. It turns out to be strong enough to produce an almost exact parallel alignment of the 3d magnetic moments at low temperature. This interaction primarily governs the temperature dependence of the 3d moment and the Curie temperature, T_C, of a 3d–4f compound. The R–M interaction essentially determines the magnetic behavior of the rare-earth sublattice. Due to the localized character of the 4f shell, these R–M interactions are indirect, mediated by the 5d, 6s conduction electrons. The 3d–4f interaction produces a dominant contribution to the molecular field experienced by the rare-earth moments. The R–R interaction between the 4f spins is generally the weakest one in the 3d–4f compounds [1,2].

The R_2Fe_{17} compounds are not suitable for permanent magnet materials, because the magnetic anisotropy is planar. The substitution of nonmagnetic atoms, Ga, Al and Si, for Fe in R_2Fe_{17} has a profound influence on the magnetic properties, especially on determining the easy magnetization direction [3–5].

For $R_2Fe_{17-x}Ga_x$ (R = Y, Sm, Gd, Tb, Ho and Tm), the values of T_C first strongly increase with the Ga concentration in spite of the decrease in the value of μ_{Fe} and go through a maximum value, then decrease with x [6–11]. Moreover, it is surprising that T_C increases again at a higher Ga concentration ($x > 6$) for $R_2Fe_{17-x}Ga_x$ (R = Ho and Tm) and ($x > 7$) for $Y_2Fe_{17-x}Ga_x$.

By Ga substitution for Fe, the magnetic anisotropy at room temperature changes from planar to axial [3]. An uniaxial anisotropy at room temperature in $R_2Fe_{17-x}Ga_x$ is shown with high Ga concentration, $5 \leqslant x \leqslant 8$ for R = Tm and Dy, $6 \leqslant x \leqslant 8$ for R = Y, Gd and Tm and $7 \leqslant x \leqslant 8$ for R = Er. Whereas for R = Sm, the magnetic anisotropy is planar for $0 \leqslant x \leqslant 1$ and $6 \leqslant x \leqslant 8$ and axial

*Fax: +81 263 47 8068.
E-mail address: fmaruya@shinshu-u.ac.jp.

0022-4596/$ - see front matter © 2005 Elsevier Inc. All rights reserved.
doi:10.1016/j.jssc.2005.07.004

for $2 \leqslant x \leqslant 5$. For $Y_2Fe_{10}Ga_7$, the Ga atoms occupy at the 6*c*, 9*d*, 18*h* and 18*f* sites with the occupation ratio, 0.80, 0, 0.25 and 0.65, respectively [12]. For $Y_2Fe_{12}Ga_5$, the Ga atoms occupy at the 6*c*, 9*d*, 18*h* and 18*f* sites with the occupation ratio, 0, 0, 0.42 and 0.40, respectively [12].

Hence, the magnetic properties of $R_2Fe_{17-x}Ga_x$ are very interesting. Here, to compare the strength of the exchange interactions between Fe spins and between *R* and Fe spins for $R_2Fe_{17-x}Ga_x$ (R = Y, Sm, Gd, Tb, Ho and Tm), we calculated the molecular field coefficients, n_{FeFe} and n_{RFe} (R = Sm, Gd, Tb, Ho and Tm), for $R_2Fe_{17-x}Ga_x$ using the experimental values of T_C. We also calculated the values of n_{FeFe} and n_{SmFe} for $Y_2Fe_{17-x}Ga_x$ $R_2Fe_{17-x}T_x$ (T = Al and Si).

2. Results and discussion

The dependence of T_C on the Ga concentration for $R_2Fe_{17-x}Ga_x$ (R = Y, Ce, Sm, Gd, Tb, Ho and Tm) is shown in Fig. 1. The values of T_C for $R_2Fe_{17-x}Ga_x$ (R = Y, Ce, Sm, Gd, Tb, Ho and Tm) are taken from Refs. [6–11,13], respectively. The values of T_C first increase and decrease, but it is surprising that those of T_C increase again at a higher Ga concentration ($x > 6$) for $R_2Fe_{17-x}Ga_x$ (R = Ho and Tm) and ($x > 7$) for $Y_2Fe_{17-x}Ga_x$. For R_2Fe_{17}, the 6*c*–6*c* and the 9*d*–18*f* pairs have negative exchange interactions. This leads to a rather low Curie temperature for R_2Fe_{17} [14]. When Ga ions preferentially occupy the 18*f* site, the negative interaction of 9*d*–18*f* sites is decreased and the total interaction is therefore enhanced and the Curie temperature increases. On the other hand, more substitution of Ga ions leads to the rapid decrease in positive interaction and the Curie temperature decreases at high substitution. The dependence of the value of μ_{Fe} on the Ga concentration for $Y_2Fe_{17-x}T_x$ (T = Ga [6], Al [15] and Si [16]) at 1.5, 4.2 and 1.5 K, respectively, is also shown in Fig. 1. The values of μ_{Fe} decrease a little with the Ga content compared with those of μ_{Co} at 4.2 K for $Gd_2Co_{17-x}Ga_x$ obtained from the saturation magnetization [17] assuming that the Gd moment is 7.0 μ_B and couples with the Fe moment ferrimagneticaly. The values of μ_{Co} decrease largely. The value of T_C is found to decrease monotonically from 1210 K for $x = 0$–30 K for $X = 8$ in $Gd_2Co_{17-x}Ga_x$ [17].

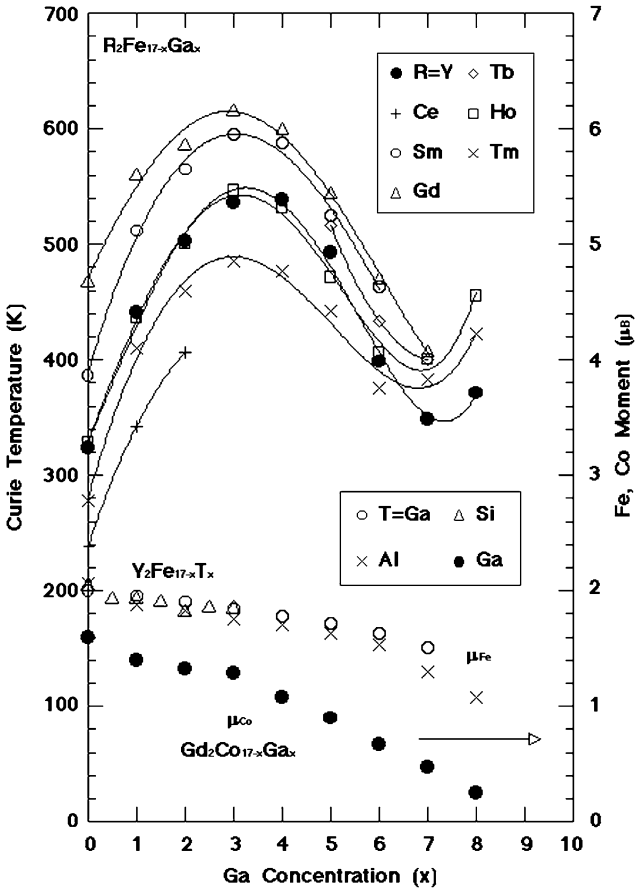

Fig. 1. The dependence of the Curie temperature, T_C, on the Ga concentration for $R_2Fe_{17-x}Ga_x$ (R = Y, Ce, Sm, Gd, Tb, Ho and Tm). The dependence of the value of μ_{Fe} on the Ga concentration for $Y_2Fe_{17-x}T_x$ (T = Ga, Al and Si) is also shown.

The dependence of the unit cell volume, *V*, on the Ga concentration for $R_2Fe_{17-x}Ga_x$ (R = Y, Sm, Gd, Tb, Ho and Tm) is shown in Fig. 2. The values of *V* for $R_2Fe_{17-x}Ga_x$ (R = Y, Sm, Gd, Tb, Ho and Tm) are taken from Refs. [6–8,10,11,18,19], respectively. The R_2Fe_{17} compounds have hexagonal and rhombohedral structures. Hence, in the case of hexa. structure, we multiply the values of *V* by 3/2 to compare the values of *V* in both structures. The values of *V* increase linearly with the Ga content. The increase in *V* for $Y_2Fe_{17-x}Ga_x$ is close to that for $Gd_2Co_{17-x}Ga_x$ [17].

The exchange interactions can be analyzed by the molecular field model, which is commonly used to describe the variation of the Curie temperature in the *R*–Fe intermetallic series, under the assumption that the localized 3*d*-electron model is applicable.

Applying the two-sublattice molecular field model to the paramagnetic state [1], the following expression can be obtained:

$$T_C = [T_{Fe} + T_R + \{(T_{Fe} - T_R)^2 + 4T_{RFe}^2\}^{1/2}]/2, \quad (1)$$

where

$$T_{Fe} = n_{FeFe} C_{Fe}, \quad (2)$$

$$T_R = \alpha^2 n_{RR} C_R \quad (3)$$

and

$$T_{RFe} = |\alpha| n_{RFe} (C_R C_{Fe})^{1/2} = \{(T_C - T_{Fe})(T_C - T_R)\}^{1/2}. \quad (4)$$

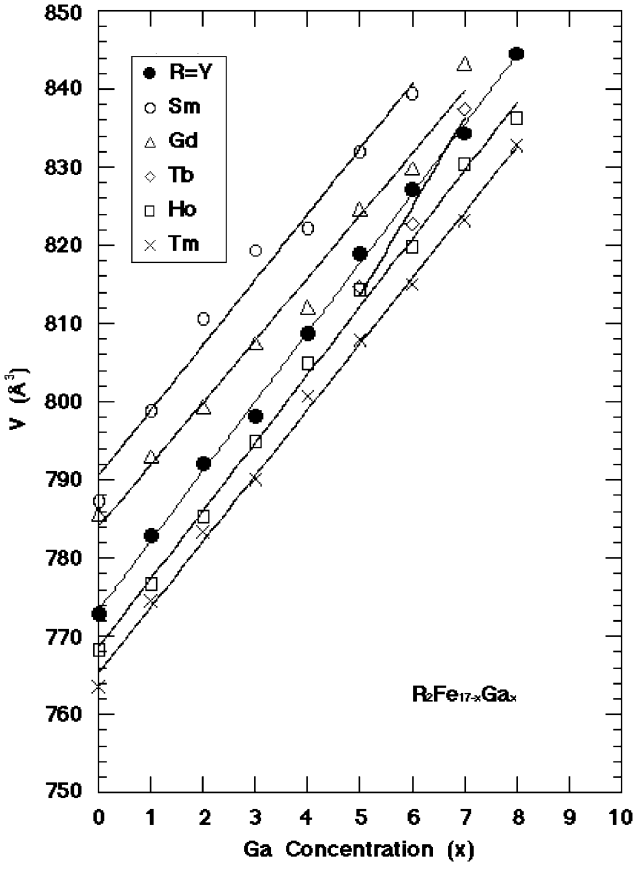

Fig. 2. The dependence of the unit cell volume, V, on the Ga concentration for $R_2Fe_{17-x}Ga_x$ (R = Y, Sm, Gd, Tb, Ho and Tm).

Here n_{ij} represents the molecular field coefficients, $C_R = N_R g^2 J(J+1)\mu_B^2/3k_B$, N_R is the number of rare-earth atoms per unit volume, $C_{Fe} = N_{Fe}4S(S+1)\mu_B^2/3k_B$, N_{Fe} is the number of Fe atoms per unit volume and $\alpha = 2(g-1)/g$. Neglecting T_R, T_C is given by

$$T_C = \{T_{Fe} + (T_{Fe}^2 + 4T_{RFe}^2)^{1/2}\}/2 \quad (5)$$

and, n_{FeFe} and n_{RFe} can be calculated using

$$n_{FeFe} = T_{Fe}/C_{Fe} \quad (6)$$

and

$$n_{RFe} = \{T_C(T_C - T_{Fe})/C_R C_{Fe}\}^{1/2}/|\alpha|, \quad (7)$$

respectively.

Here, we calculated the molecular field coefficients, n_{FeFe} and n_{RFe}, for $R_2Fe_{17-x}Ga_x$ (R = Y, Sm, Gd, Tb, Ho and Tm) using the experimental values of T_C. Taking the value of T_C for the Y compound as T_{Fe}, n_{FeFe} can be deduced using Eq. (6). Then n_{RFe} can be obtained by substituting the appropriate T_C data of each rare-earth compound into Eq. (7).

The dependence of n_{FeFe} and n_{RFe} (R = Sm, Gd, Tb, Ho and Tm) on the Ga concentration for $R_2Fe_{17-x}Ga_x$ is shown in Fig. 3. The values of n_{FeFe} increase in spite of

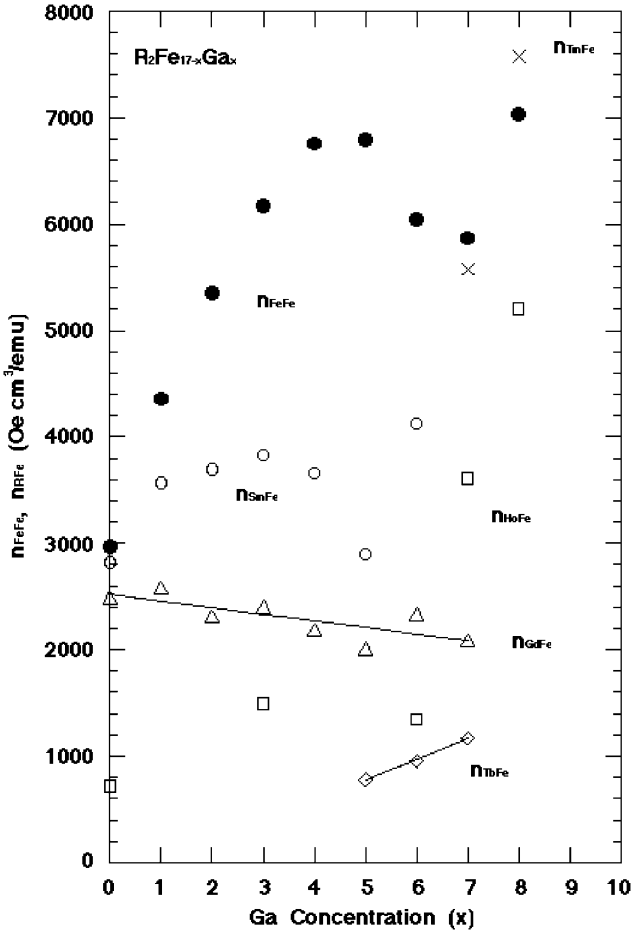

Fig. 3. The dependence of n_{FeFe} and n_{RFe} (R = Sm, Gd, Tb, Ho and Tm) on the Ga concentration for $R_2Fe_{17-x}Ga_x$.

the decrease of μ_{Fe} for $0 \leqslant x \leqslant 5$. The values of n_{SmFe} have large values when the magnetic anisotropy is axial. For $0 \leqslant x \leqslant 6$, the values of n_{SmFe} are largest among those of n_{RFe}. The values of n_{GdFe} decrease with the Ga concentration. The values of n_{FeFe} are larger than those of n_{RFe}. The value of n_{RR} deduced from the ordering temperature for R–Ni compounds is 226 (Oe cm^3/emu) [1]. That is much smaller than the calculated n_{FeFe} and n_{RFe} (R = Sm, Gd, Tb, Ho and Tm) values for $R_2Fe_{17-x}Ga_x$. For $6 \leqslant x \leqslant 8$, the values of n_{FeFe}, n_{HoFe} and n_{TmFe} increase largely, which is related to the change of the easy magnetization direction.

The total magnetocrystalline anisotropy constant is the sum of the first-order anisotropy constants of the rare earth, R, and iron sublattices,

$$K_1(\text{total}) = K_1(\text{Fe}) + K_1(R). \quad (8)$$

where K_1 (Fe) and K_1 (R) are the anisotropy constants of the Fe sublattice and the rare earth one, respectively. K_1 (Fe) is negative for R_2Fe_{17} compounds [20]. At room temperature, the rare-earth sublattice anisotropy is too small to overcome the iron easy plane anisotropy. K_1 (R)

can be expressed [21] in crystal field terms as

$$K_1(R) = -3/2B_2^0\langle O_2^0\rangle \quad (9)$$

and

$$B_2^0 = \alpha_J\langle r^2\rangle A_2^0, \quad (10)$$

where B_2^0 is the second-order crystal field interaction, which represent the interactions of a 4*f* ion with the surrounding electronic charges. α_J is the Stevens coefficient and A_2^0 is the second-order crystal field parameter, which is determined predominantly by the rare-earth valence electron charge asphericity [22]. A_2^0 is strongly influenced by the variation of x in $R_2Fe_{17-x}Ga_x$, because of the hybridization of the rare-earth 5*d* and 6*p* valence electrons with the valence electrons of its neighboring atoms [18]. α_J for Sm, Er and Tm is positive. α_J for Pr, Nd, Tb, Dy and Ho is negative. α_J for Gd is zero. In the rhombohedral R_2Fe_{17} compounds A_2^0 is small and negative [17]. An uniaxial anisotropy at room temperature is shown in $Sm_2Fe_{17-x}Ga_x$ for $2 \leqslant x \leqslant 5$. For $Sm_2Fe_{17-x}Ga_x$, $K_1(R)$ is positive and Ga substitution results in the increase in magnitude of A_2^0 and hence $K_1(R)$. So, with low Ga concentration, the magnetic anisotropy changes from planar to axial. An uniaxial anisotropy at room temperature is shown in $R_2Fe_{17-x}Ga_x$ (R = Y and Gd) with high Ga concentration for $6 \leqslant x \leqslant 8$. Hence, the increase in the uniaxial anisotropy is probably due to the reduction in the planar anisotropy of the Fe sublattice with Ga substitution. An uniaxial anisotropy at room temperature in $R_2Fe_{17-x}Ga_x$ (R = Tb, Dy, Ho, Er and Tm) with high Ga concentration for $x \geqslant 6$ is due to the changes of the magnitude and sign of the rare earth valence electron asphericity, A_2^0, and the reduction in the planar anisotropy of the Fe sublattice.

The dependence of n_{FeFe}/n_{RFe} (R = Sm, Gd, Tb, Ho and Tm) on the Ga concentration for $R_2Fe_{17-x}Ga_x$ is shown in Fig. 4. The values of n_{FeFe}/n_{RFe} for R = Sm and Tm, whose α_J is positive, are small, so the contributions of the *R*–*M* interaction are large. For $6 \leqslant x \leqslant 7$ the values of n_{FeFe}/n_{RFe} for R = Ho and Tb, whose α_J is negative, decrease largely, so the contributions of the *R*–*M* interaction become large, which is related to the change of magnetic anisotropy. The value of n_{CoCo} is 18 times larger than that of n_{GdCo} for Gd_2Co_{17} [23]. On the contrary, the values of n_{FeFe} are 1.2–3.4 times larger than those of n_{GdFe} for $Gd_2Fe_{17-x}Ga_x$. The *R*–Co exchange is negligible compared with the strong Co–Co exchange, but the *R*–Fe exchange is significant compared to the Fe–Fe exchange.

The values of n_{FeFe} and n_{RFe} (R = Sm, Gd, Tb, Ho and Tm) plotted versus the corresponding reciprocal values of the unit cell volume, V^{-1}, for $R_2Fe_{17-x}Ga_x$ (R = Y, Sm, Gd, Tb, Ho and Tm) are shown in Fig. 5. The values of n_{FeFe} have a maximum value. The values of n_{RFe} almost decrease with increasing V^{-1} except for

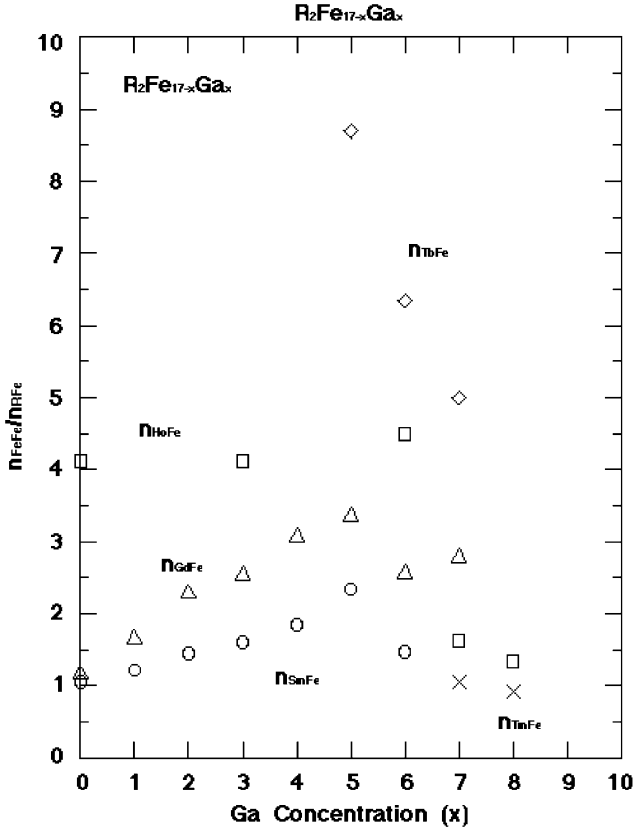

Fig. 4. The dependence of n_{FeFe}/n_{RFe} (R = Sm, Gd, Tb, Ho and Tm) on the Ga concentration for $R_2Fe_{17-x}Ga_x$.

those of n_{GdFe}. The values of n_{GdFe} increase with increasing those of V^{-1}. The change in the values of n_{FeFe} and n_{HoFe} is large.

In rare-earth–transition metal compounds, the exchange coupling of localized 4*f* and itinerant 3*d* moments is indirectly promoted via a local 4*f*–5*d* interaction combined with an interatomic 5*d*–3*d* interaction [24]. The 2*p* electrons of Ga lower the density of 3*d* states at the Fermi level by the 3*d*–2*p* hybridization [25] and the values of Fe 3*d* moment decrease, which reduces the effect of 5*d*–3*d* hybridization and weakens the 4*f*–3*d* exchange interaction. Consequently, with increasing Ga content the values of μ_{Fe} decrease and those of n_{RFe} decrease. But, the values of n_{RFe} increase except for n_{GdFe} with decreasing μ_{Fe}, which is very surprising.

The reductions of μ_{Fe} for $Y_2Fe_{17-x}T_x$ (T = Ga, Al and Si) by Ga, Al and Si substitution are similar as shown in Fig. 1, which indicates that the Fe–Ga, Fe–Al and Fe–Si electronic hybridizations are also similar. The valence electrons of B, Al, Si and Ga are $2s^2sp^1$, $3s^23p^1$, $3s^23p^2$ and $4s^24p^1$, respectively and these atoms have the similar valence electron configurations. The reduction of μ_{Fe} by Ga substitution is smaller than that of μ_{Co} for $Gd_2Co_{17-x}Ga_x$. This indicates that the Co–Ga electronic hybridization is more effective than that of Fe–Ga.

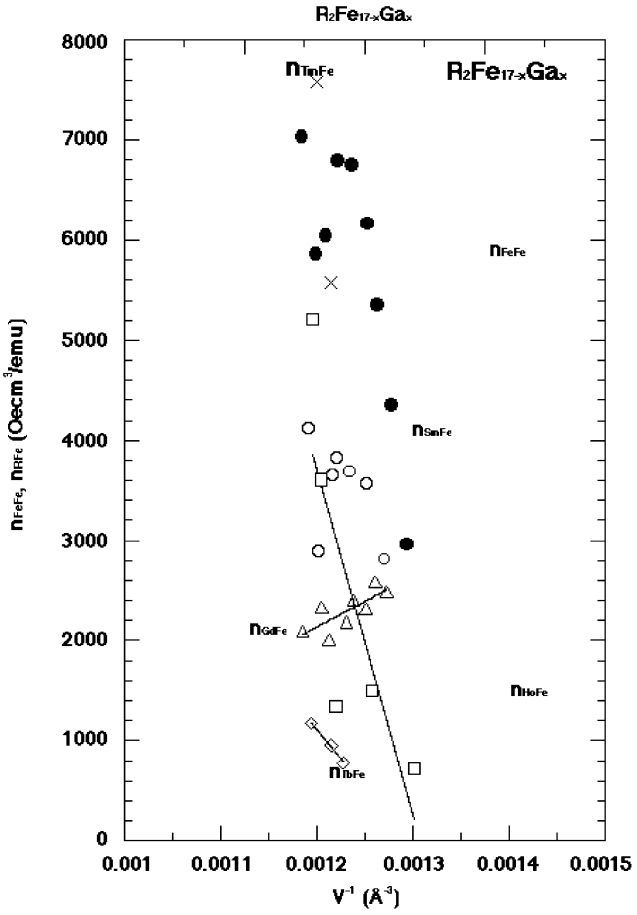

Fig. 5. The values of n_{FeFe} and n_{RFe} (R = Sm, Gd, Tb, Ho and Tm) plotted versus the corresponding reciprocal values of the unit cell volume, V^{-1}, for $R_2Fe_{17-x}Ga_x$ (R = Y, Sm, Gd, Tb, Ho and Tm).

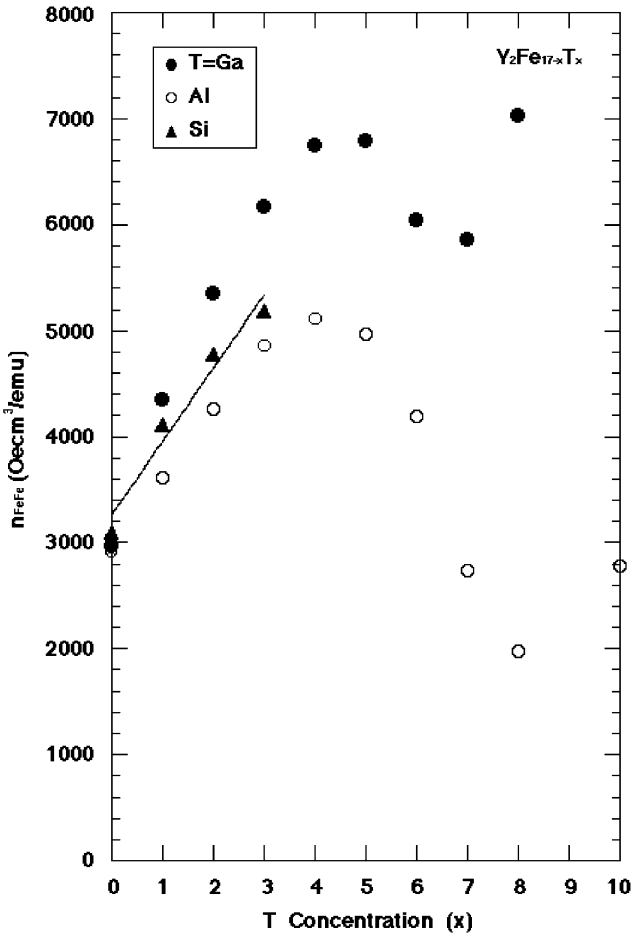

Fig. 6. The dependence of n_{FeFe} on the T concentration for $Y_2Fe_{17-x}T_x$ (T = Ga, Al and Si).

The reduction of μ_{Co} by Ga substitution is smaller than that by B substitution in spite of the similar valence electron configurations of Ga and B [26]. This indicates that the Co–B electronic hybridization is more effective than that of Co–Ga. We studied the Co–B electronic hybridization for 2–17 and 2–14 rare-earth Co compounds previously [27].

The values of n_{ErCo} for $ErCo_3$, Er_2Co_7, $ErCo_4B$, $ErCo_{5.8}$, $Er_2Co_{14}B$, Er_2Co_{17} and $ErCo_{12}B_6$ are roughly proportional to those of V^{-1}, where V is the unit cell volume, and this has been explained by assuming that with decreasing V, the 5*d*–3*d* hybridization increases and the 4*f*–3*d* exchange interaction increases [28]. Consequently, if the value of V decreases, that of n_{RFe} increases. The change of the values of n_{GdFe} is only explained by the above reason.

The dependence of n_{FeFe} on the T concentration for $Y_2Fe_{17-x}T_x$ (T = Ga, Al and Si) is shown in Fig. 6. For $Y_2Fe_{17-x}T_x$ (T = Ga and Al), the values of n_{FeFe} increase and have large values around $x = 3$–4 with increasing the Ga content. The vales of n_{FeFe} for $Y_2Fe_{17-x}Al_x$ decrease largely, which is due to the large decrease of μ_{Fe}. The values of n_{FeFe} are large when x is 4–5. The values of n_{FeFe} for $Y_2Fe_{17-x}Si_x$ also increase for $0 \leqslant x \leqslant 3$, nevertheless those of V decrease. The values of V decrease with the Ga content, which can be related to a steric effect due to the smaller covalent radius of Si.

A plot of n_{FeFe} versus μ_{Fe} for $Y_2Fe_{17-x}T_x$ (T = Ga, Al and Si) is shown in Fig. 7. For $Y_2Fe_{17-x}T_x$ (T = Ga and Al), the values of n_{FeFe} have a maximum value when μ_{Fe} is 1.7 μ_B. The values of n_{FeFe} depend on those of μ_{Fe}. For Y–Co–B compounds, YCo_5, Y_2Co_{17}, $Y_2Co_{14}B$, YCo_4B, $Y_3Co_{11}B_4$ and $Y_2Co_7B_3$ [28], the values of n_{CoCo} increase with increasing those of μ_{Co}.

The values of n_{FeFe} plotted versus the corresponding reciprocal values of the unit cell volume, V^{-1}, for $Y_2Fe_{17-x}T_x$ (T = Ga, Al and Si) are shown in Fig. 8. For $Y_2Fe_{17-x}T_x$ (T = Ga and Al), the values of n_{FeFe} have a maximum value around the same value of V^{-1}. For $Y_2Fe_{17-x}Si_x$, the values of n_{FeFe} increase with increasing V^{-1}.

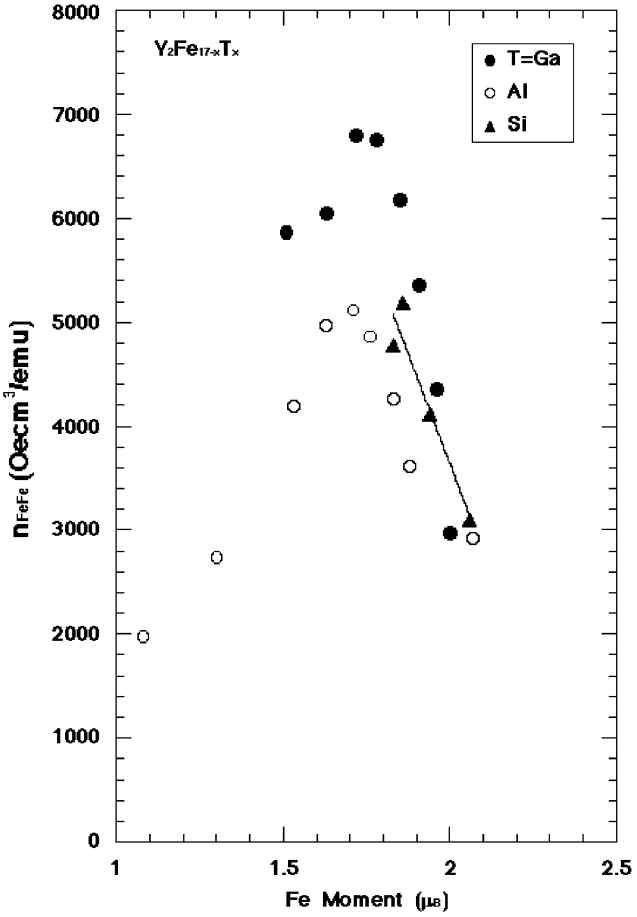

Fig. 7. A plot of n_{FeFe} versus μ_{Fe} for $Y_2Fe_{17-x}T_x$ (T = Ga, Al and Si).

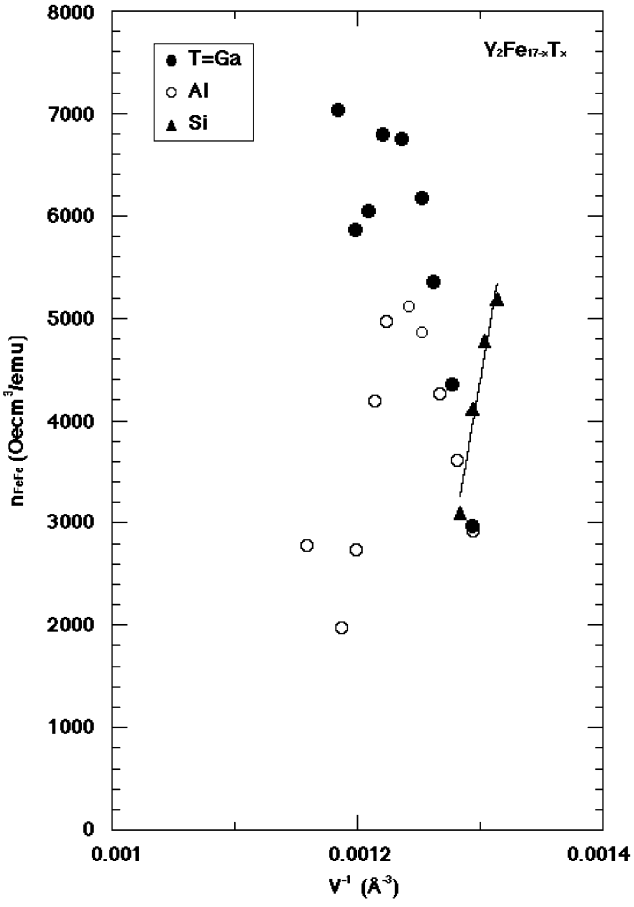

Fig. 8. The values of n_{FeFe} plotted versus the corresponding reciprocal values of the unit cell volume, V^{-1}, for $Y_2Fe_{17-x}T_x$ (T = Ga, Al and Si).

With increasing the value of $V^{1/3}$, the values of μ_{Fe} for $Y_2Fe_{17-x}T_x$ (T = Ga and Al) decrease and those for T = Si increase. Especially, those for T = Al decrease largely. In Y–Co–B compounds, YCo_5, Y_2Co_{17}, $Y_2Co_{14}B$, YCo_4B, $Y_3Co_{11}B_4$ and $Y_2Co_7B_3$ [29], the values of μ_{Co} are apparently proportional to those of the cube root of V. These results suggest that the values of μ_{Co} are proportional to the atomic distances.

3. Conclusions

(1) The values of n_{FeFe} increase in spite of the decrease of μ_{Fe} for $0 \leqslant x \leqslant 5$. The values of n_{SmFe} have large values when the magnetic anisotropy is axial. For $6 \leqslant x \leqslant 8$, the values of n_{FeFe}, n_{HoFe} and n_{TmFe} increase largely, which is related to the change of the easy magnetization direction.

(2) The reductions of μ_{Fe} for $Y_2Fe_{17-x}T_x$ (T = Ga, Al and Si) by Ga substitution are similar, which indicates that the Fe–Ga, Fe–Al and Fe–Si electronic hybridizations are also similar.

(3) For $Y_2Fe_{17-x}T_x$ (T = Ga and Al), the values of n_{FeFe} have a maximum value with increasing those of μ_{Fe} and depend on those of μ_{Fe}. With increasing V^{-1}, the values of n_{FeFe} have a maximum value around the same value of V^{-1} for $Y_2Fe_{17-x}T_x$ (T = Ga and Al). For $Y_2Fe_{17-x}Si_x$, the values of n_{FeFe} increase with increasing V^{-1}.

References

[1] E. Belorizky, M.A. Fremy, J.P. Gavigan, D. Givord, H.S. Li, J. Appl. Phys. 61 (1987) 3971.
[2] J.J.M. Franse, R.J. Radwanski, in: K.H.J. Buschow (Ed.), Handbook of Magnetic Materials, vol. 7, North-Holland, Amsterdam, 1993, p. 307.
[3] B.G. Shen, Z.H. Cheng, B. Liang, H.Q. Guo, J.X. Zhang, H.Y. Gong, F.W. Wang, Q.W. Yan, W.S. Zhan, Appl. Phys. Lett. 67 (1995) 1621.
[4] Z. Wang, R.A. Dunlap, J. Phys.: Condens. Matter 5 (1993) 2407.
[5] B.G. Shen, B. Liang, F.W. Wang, Z.H. Cheng, H.Y. Gong, S.Y. Zhang, J.X. Zhang, J. Appl. Phys. 77 (1995) 2637.
[6] B.G. Shen, Z.H. Cheng, H.Y. Gong, B. Liang, Q.W. Yan, F.W. Wang, J.X. Zhang, S.Y. Zhang, H.Q. Guo, J. Alloy Compd. 226 (1995) 51.
[7] B.G. Shen, F.W. Wang, L.S. Kong, L. Cao, J. Phys.: Condens. Matter 5 (1993) L685.

[8] Z.H. Cheng, B.G. Shen, B. Liang, J.X. Zhang, F.W. Wang, S.Y. Zhang, J.G. Zhao, W.S. Zhan, J. Appl. Phys. 78 (1995) 1385.
[9] Y. Hao, J. Magn. Magn. Mater. 214 (2000) 119.
[10] F. Wang, B.G. Shen, P. Zhng, Z.H. Cheng, J. Zhang, H. Gong, B. Liang, X. Sun, Q. Yan, J. Appl. Phys. 83 (1998) 3250.
[11] B.G. Shen, Z.H. Cheng, F.W. Wang, Q.W. Tan, H. Tang, B. Liang, S.Y. Zhang, F.R. de Boer, K.H.J. Buschow, S. Ridwan, J. Appl. Phys. 83 (1998) 5945.
[12] Q.W. Yan, P.L. Zhang, X.D. Shen, B.G. Chen, Z.H. Cheg, C. Gou, D.F. Chen, Ridwan, Mujamilah, Gunawan and Marsongkohadi, J. Phys.: Condens. Matter. 8 (1996) 1485.
[13] H. Luo, Z. Hu, W.B. Yelon, S.R. Mishra, G.J. Long, O.A. Pringle, D.P. Middleton, K.H.J. Buschow, J. Appl. Phys. 79 (1996) 6318.
[14] Z.W. Li, A.H. Morrish, Phys. Rev. B 55 (1997) 3670.
[15] T.H. Jacobs, K.H.J. Buschow, G.F. Zhou, X. Li, F.R. de Boer, J. Magn. Magn. Mater. 116 (1992) 220.
[16] C. Lin, Y.X. Sun, Z.X. Liu, H.W. Jiang, G. Jiang, J.L. Yang, B.S. Zhang, Y.F. Ding, Solid State Commun. 81 (1992) 299.
[17] B. Liang, B.G. Shen, F.W. Wang, T.Y. Zhao, Z.H. Cheng, S.Y. Zhang, H.Y. Gong, W.S. Zhan, J. Appl. Phys. 82 (1997) 3452.
[18] Z. Hu, W.B. Yelon, S. Mishra, G.J. Long, O.A. Pringle, D.P. Middleton, K.H.J. Buschow, F. Grandjean, J. Appl. Phys. 76 (1994) 443.
[19] O.A. Pringle, G.J. Long, S.R. Mishra, D. Hautot, F. Grandjean, D.P. Middleton, K.H.J. Buschow, Z. Hu, H. Luo, W.B. Yelon, J. Magn. Magn. Mater. 183 (1998) 81.
[20] K.H.J. Buschow, Rep. Prog. Phys. 54 (1991) 1123.
[21] C. Rudowics, J. Phys. C 18 (1985) 1415.
[22] R. Coehoorn, K.H.J. Buschow, J. Appl. Phys. 69 (1991) 5590.
[23] R.J. Radwanski, Physica B 142 (1986) 57.
[24] M.S.S. Brooks, O. Eriksson, B. Johanson, J. Phys.: Condens. Matter 1 (1989) 5861.
[25] M. Aoki, H. Yamada, Physica B 177 (1992) 259.
[26] C. Zlotea, O. Isnard, J. Alloys Compd. 346 (2002) 29.
[27] F. Maruyama, H. Nagai, Y. Amako, H. Yoshie, K. Adachi, Jpn. J. Appl. Phys. 35 (1996) 6057.
[28] J.P. Liu, F.R. de Boer, P.F. de Chatel, R. Coehoorn, K.H.J. Buschow, J. Magn. Magn. Mater. 132 (1994) 159.
[29] F. Maruyama, J. Alloys Compd. 320 (2001) 7.